This is the author's version of a work that was submitted/accepted for publication in the following source:

Kaminskas, Lisa M., McLeod, Victoria M., Ascher, David B., Ryan, Gemma M., Jones, Seth, Haynes, John M., Trevaskis, Natalie L., Chan, Linda J., Sloan, Erica K., Finnin, Benjamin A., Williamson, Mark, Velkov, Tony, Williams, Elizabeth D., Kelly, Brian D., Owen, David J., & Porter, Christopher J.H.

Methotrexate-conjugated PEGylated dendrimers show differential patterns of deposition and activity in tumour-burdened lymph nodes after intravenous and subcutaneous administration in rats

Lisa M Kaminskas[a*†], Victoria M McLeod[a†], David B Ascher[b], Gemma M Ryan[a], Seth Jones[a], John M Haynes[c], Natalie L Trevaskis[a], Linda J Chan[a], Erica K Sloan[c], Benjamin A Finnin[c], Mark Williamson[d], Tony Velkov[a], Elizabeth D Williams[e], Brian D Kelly[f], David J Owen[f], Christopher JH Porter[a*]

[a] Drug Delivery Disposition and Dynamics Group, Monash Institute of Pharmaceutical Sciences, Monash University, Parkville, VIC, Australia, 3052

[b] ACRF Rational Drug Discovery centre and Biota Structural Biology Laboratory, St Vincent's Institute for Medical Research, Fitzroy, VIC, Australia, 3000

[c] Drug Discovery Biology, Monash Institute of Pharmaceutical Sciences, Monash University, Parkville, VIC, Australia, 3052

[d] Gribbles Veterinary Pathology, Clayton, VIC, Australia, 3168

[e] Australian Prostate Cancer Research Centre, Institute of Health and Biomedical Innovation, Queensland University of Technology, Brisbane, QLD, Australia, 4102; Department of Surgery, St Vincent's Hospital, The University of Melbourne, Fitzroy, VIC, Australia, 3065; Monash Institute of Medical Research, Monash University, Clayton, VIC, Australia, 3168

[f] Starpharma Pty Ltd, Melbourne, VIC, Australia, 3004.

† these authors contributed equally to this manuscript

Keywords: methotrexate, lymphatic, lymphatic metastasis, pharmacokinetics, subcutaneous, dendrimer

*Corresponding authors:

Dr Lisa M Kaminskas   Prof Christopher JH Porter

Monash Institute of Pharmaceutical Sciences   Monash Institute of Pharmaceutical Sciences

381 Royal Pde, Parkville   381 Royal Pde, Parkville

VIC, Australia, 3052   VIC, Australia, 3052

Ph. +61 3 9903 9522   Ph. +61 3 9903 9649

Fax. +61 3 9903 9583   Fax. +61 3 9903 9583

Email. lisa.kaminskas@monash.edu   Email. chris.porter@monash.edu

1

For table of contents use only:

Methotrexate-conjugated PEGylated dendrimers show differential patterns of deposition and activity in tumour-burdened lymph nodes after intravenous and subcutaneous administration in rats

Lisa M Kaminskas[a*†], Victoria M McLeod[a†], David B Ascher[b], Gemma M Ryan[a], Seth Jones[a], John M Haynes[c], Natalie L Trevaskis[a], Linda J Chan[a], Erica K Sloan[c], Benjamin A Finnin[c], Mark Williamson[d], Tony Velkov[a], Elizabeth D Williams[e], Brian D Kelly[f], David J Owen[f], Christopher JH Porter[a*]

Abstract:

The current study sought to explore whether the subcutaneous administration of lymph-targeted dendrimers, conjugated with a model chemotherapeutic (methotrexate, MTX), was able to enhance anticancer activity against lymph node metastases. The lymphatic pharmacokinetics and antitumour activity of PEGylated polylysine dendrimers conjugated to MTX [D-MTX(OH)] via a tumour-labile hexapeptide linker was examined in rats and compared to a similar system where MTX was α-carboxyl O-*tert*-butylated [D-MTX(OtBu)]. The latter has previously been shown to exhibit longer plasma circulation times. D-MTX(OtBu) was well absorbed from the subcutaneous injection site via the lymph, and 3 to 4%/g of the dose was retained by sentinel lymph nodes. In contrast, D-MTX(OH) showed limited absorption from the subcutaneous injection site, but absorption was almost exclusively via the lymph. The retention of D-MTX(OH) by sentinel lymph nodes was also significantly elevated (approximately 30% dose/g). MTX alone was not absorbed into the lymph. All dendrimers displayed lower lymph node targeting after intravenous administration. Despite significant differences in the lymph node retention of D-MTX(OH) and D-MTX(OtBu) after subcutaneous and intravenous administration, the growth of lymph node metastases was similarly inhibited. In contrast, the administration of MTX alone did not significantly reduce lymph node tumour growth. Subcutaneous administration of drug-conjugated dendrimers therefore provides an opportunity to improve drug deposition in downstream tumour-burdened lymph nodes. In this case, however, increased lymph node biodistribution did not correlate well with antitumour activity, possibly suggesting constrained drug release at the site of action.

3

Introduction:

The metastatic spread of solid tumours is responsible for approximately 90% of all cancer-related deaths.[1] Metastasis may occur either via the blood (leading to secondary tumour development in target organs such as the lungs, bone marrow and brain) or via the lymph (leading initially to the development of tumours in the sentinel lymph nodes draining the primary tumour). Metastases are commonly treated via a combination of surgical removal and chemo- and radiation-therapies.[2] The surgical removal of tumour-bearing sentinel lymph nodes (lymphadenectomy), however, has only limited success in preventing the subsequent spread of the cancer.[3-6] This has been suggested to reflect the realisation that 1) cancer cells that have passed beyond the sentinel nodes or are in transit to downstream lymph nodes are not removed during lymphadenectomy, 2) an intact lymphatic system may enhance the eradication of metastasising cancer cells[7] and therefore lymph node removal may inhibit metastatic clearance, and 3) post lymphadectomy, metastatic pathways via the blood remain intact and are promoted by metastatic cancers releasing factors that prime key target organs.[8, 9] As such, the potential for ongoing metastatic spread remains. Whilst post-surgical chemotherapy has the potential to target and kill cancer cells that have metastasised beyond the sentinel lymph nodes, small molecule cancer chemotherapy drugs display limited lymphatic availability after intravenous (IV) and subcutaneous (SC) administration.[10] The combined treatment of lymphatic metastases with surgery and lymph-targeted chemotherapeutic nanomedicines may therefore improve outcomes for cancers that metastasise via the lymph.

Several liposomal, nanoparticulate and polymeric nanomedicines are currently in the clinic or in clinical trials as tumour-targeted drug delivery systems. These are almost exclusively administered IV to enhance drug exposure to solid tumours via the enhanced permeation and retention (EPR) effect.[11-13] Previous work in our laboratory, however, has shown that long circulating PEGylated nanomaterials such as PEGylated liposomal doxorubicin (100 nm, marketed as Doxil® or Caelyx®) and a 56 kDa doxorubicin-loaded PEGylated dendrimer (12 nm) readily access the lymph after SC delivery and might assist in gaining access to sites of lymphatic metastasis.[10] SC administration at the site of a primary tumour offers the potential advantage of higher drug concentrations in the lymphatics draining the injection site (when compared to IV administration), selective targeting to downstream lymph nodes, and reduced drug concentrations in blood (and therefore reduced systemic toxicity).[14] We have previously shown that PEGylated dendrimers larger than approximately 20 kDa are preferentially absorbed from interstitial injection sites via the lymph and are retained by sentinel lymph nodes in a size dependent manner (where larger dendrimers display better lymph node retention than smaller dendrimers).[15] In this study, a 12 nm doxorubicin-conjugated PEGylated polylysine dendrimer was shown to target the lymphatics after SC administration and to be retained within lymph nodes more effectively than either a 100

4

nm PEGylated liposomal formulation or a simple solution formulation of doxorubicin.[10] This suggests that dendrimers have the potential to enhance drug exposure to lymph node-resident metastases when compared to commercially available solution and liposomal formulations.

In this previous study, retention of the doxorubicin-conjugated dendrimer in lymph nodes was suggested to occur via physical entrapment of the polymer within lymph nodes. This strategy may be further enhanced by employing drug carriers that target lymph node-resident macrophages.[16-19] This can be accomplished via the conjugation of macrophage targeting ligands, such as mannose, to the carrier surface, or by increasing surface charge to promote recognition of the carrier by both the lymph node parenchyma and lymph node-resident macrophages.

In this regard, we have recently characterised the IV pharmacokinetics of two 69-71 kDa methotrexate (MTX)-conjugated PEGylated polylysine dendrimers (Figure 1) that display significant differences in charge, macrophage targeting and pharmacokinetic and biodistribution behaviour.[20] Conjugation of MTX to the α-amino group on surface lysine residues via a matrix metalloproteinase cleavable PVGLIG (Pro-Val-Gly-Leu-Ile-Gly) linker led to rapid clearance from plasma via the organs of the mononuclear phagocyte system (MPS), in particular the liver. The scaffold was then biodegraded and monomeric lysine liberated, redistributed to the liver and incorporated into protein resynthetic pathways. As a result of rapid plasma clearance, however, the D-MTX(OH) dendrimer did not show efficient tumour targeting and chemotherapeutic activity.[20] In contrast, capping the free carboxyl group of MTX with an OtBu functionality, reduced MPS clearance and increased the plasma half-life of D-MTX(OH). The OtBu dendrimer subsequently showed efficient uptake into tumours and improved antitumour activity when compared to a solution formulation of MTX.[20]

Although D-MTX(OH) did not show anti-cancer activity in a mouse xenograft model after IV delivery in the previous study[20], the enhanced affinity of this dendrimer for the cells of the MPS suggests the possibility of enhanced uptake by macrophages in lymph nodes draining an SC injection site, and improved chemotherapeutic activity after local administration. In the present study, we therefore sought to examine this hypothesis and to compare the patterns of lymphatic disposition and antitumour activity of the two MTX-conjugated dendrimer constructs after SC and IV administration in rats. In vivo activity was expected to be a function of biodistribution towards the tumour-burdened lymph node, disposition of the drug within the node and efficient liberation of drug within the tumour. The cancer model employed involved the footpad injection of rat mammary MAT 13762 IIIB carcinoma cells into syngeneic F344 rats to generate secondary lymphatic metastases in the popliteal lymph node of fully immunocompetent rats. The cellular targets and regional distribution of D-MTX(OH) in lymph nodes was also examined via confocal fluorescence microscopy and flow cytometry.

Methods:

Materials & Reagents

The hexapeptide (PVGLIG) was purchased as a custom synthesis from EZbiolab (IN, USA). Unlabeled lysine for synthesis was from Bachem (Bunbendorf, Switzerland). (L)-(4,5-^{3}H)-Lysine (1 mCi/mL) was purchased from MP Biomedicals (CA, USA). Monodisperse NHS-PEG$_{1100}$ was obtained from Quanta BioDesign, Ltd. (USA). The NHS ester of Atto488 was obtained from Perkin Elmer (MA, USA). Methotrexate [3',5',7'-^{3}H] sodium salt was from American Radiolabelled Chemicals (St. Louis, MO, USA). Medical grade polyethylene, polyvinyl and silastic tubing (0.58 mm internal diameter, 0.96 mm external diameter) were obtained from Microtube Extrusions (NSW, Australia). RPMI Medium 1640, Dulbecco's Phosphate Buffered Saline (DPBS) without CaCl$_2$ or MgCl$_2$, fetal bovine serum (FBS), glutaMAX, penicillin/streptomycin, and 0.25% trypsin-EDTA were purchased from Gibco® (Invitrogen, VIC, Australia). Culture flasks and plates were from Corning (NY, USA). Microplates were from Greiner Bio-One (Biolab, VIC, Australia). Methotrexate, collagenase (type IV) and 3-[4,5-dimethylthiazol-2-yl]-2,5-diphenyltetrazolium bromide (MTT) were purchased from Sigma (NSW, Australia). pmCherry-C1 vector was purchased from Clontech (Mountain View, CA). Lipofectamine™ LTX and PLUS™ Reagent kit were purchased from Invitrogen (VIC, Australia). G-418 Solution (neomycin) was purchased from Roche (NSW, Australia). Soluene-350 tissue solubiliser and Irga Safe Plus liquid scintillation cocktail were purchased from Packard Biosciences (Meriden, CT). Buffer reagents (analytical reagent grade) were from Ajax Finechem Pty Ltd. (NSW, Australia). Dispase, deoxyribonuclease I, ACK Lysis Buffer and SYTOX Blue dead cell stain were from Invitrogen (VIC, Australia). GentleMACS C-tubes and M-tubes were obtained from Miltenyi Biotech Australia (NSW, Australia). All antibodies and BD Trucount tubes were purchased from Becton Dickinson (Bedford, MA). All other reagents were AR grade.

Synthesis of dendrimers

The synthesis and characterisation of the tritiated G5 dendrimer constructs containing a surface of 50% PEG$_{1100}$ and 50% underivatised primary amine or 50% cleavable hexapeptide (PVGLIG) methotrexate have been previously described.[20, 21] Briefly, generation 5 poly-L-lysine scaffolds were conjugated with methotrexate at surface α-amino groups via a PVGLIG linker and with PEG$_{1100}$ at surface ε-amino groups (Figure 1). Methotrexate contained either an OtBu-protecting group at the α-carboxyl (to give D-MTX(OtBu)) or remained unconjugated (to give D-MTX(OH)). D-MTX(OH) and D-MTX(OtBu) contained 17% MTX per weight (equivalent to approximately 26 MTX molecules per dendrimer). A control dendrimer that represented a possible

6

product of peptide cleavage and MTX liberation (where a partial positive charge would be conferred on the dendrimer; D-NH$_2$) was similarly PEGylated with PEG$_{1100}$ at surface ε-amino groups, but remained unconjugated at ε-amino groups (to give a 50:50 surface of PEG and primary amino groups). In addition, a G5 dendrimer containing 50% PEG$_{1100}$ and 50% PVGLIG where the surface proline was conjugated with glutamic acid to present a carboxylate (D-COOH) was synthesised and characterised as described in the supporting information. This provided a dendrimer with a partial anionic charge to serve as a control for D-MTX(OH)) For in vivo/in vitro imaging studies, D-MTX(OH) was prepared with 1 or 2 Atto488 fluorescent labels. This was achieved by adding 2 moles of NHS-Atto488 per mole of dendrimer scaffold during PEG conjugation.

Animals

Male Sprague Dawley (SD) rats (270-320 g) were supplied by Monash Animal Services (VIC, Australia). Female F344 rats (8-10 weeks) were supplied by Animal Resources Centre (WA, Australia). Animals were maintained on a 12 h light dark cycle and were provided with water at all times. Food was withheld only after surgical placement of cannulas and for 8 hours after dosing. All animal experimentation was approved by the institutional Animal Ethics Committee.

Cell Culture

Rat mammary MAT 13762 IIIB carcinoma cells (MAT) were purchased from ATCC (Manassas, VA) and were transfected with a vector encoding the fluorescent protein mCherry-C1 for imaging studies as described in the supporting information (supporting information available free of charge via the Internet at http://pubs.acs.org). Murine RAW-264.7 macrophages (RAW) were a kind donation by Dr Julian Quinn (Prince Henry's Institute, Melbourne). Cells were propagated in RPMI media supplemented with 10% FBS, 1% Glutamax and 100 U penicillin/ 100μg streptomycin and maintained in a 37°C humidified environment and 5% CO$_2$. MAT cells were passaged using trypsin-EDTA and RAW cells via a mechanical cell scraping method. All cells were used between passages 5 and 10 and tested negative for mycoplasma contamination. The cytotoxicity of the dendrimers and unconjugated methotrexate were tested against MAT and RAW cancer cells as well as primary rat peritoneal macrophages and rat lymphocytes that were obtained from thoracic duct lymph as described in the supporting information.

Determination of lymphatic pharmacokinetics in Sprague Dawley rats

Pharmacokinetic studies were conducted in parallel subsets of animals (n=3-4) for each dendrimer and free methotrexate to give three data sets: 1) an IV dosed control (non-lymph cannulated) group, 2) a SC dosed control (non-lymph cannulated) group and 3) a SC dosed thoracic

7

lymph duct cannulated group as previously described.[15] Rats were anaesthetised using isoflurane and cannulated via the carotid artery for blood sample collection in all groups and the right jugular vein for IV dosing or saline infusion in IV control and SC lymph cannulated groups respectively, as previously described[22]. The SC lymph group additionally had cannulas implanted in the thoracic lymph duct for continuous lymph collection using previously reported surgical procedures.[15] Following overnight recovery, rats were administered 5 mg/kg dendrimer or MTX (equating to 0.5-1 µCi of ^{3}H-dendrimer or 2-4 µCi ^{3}H-methotrexate) in 1 ml saline over a 2 minute infusion via the jugular vein cannula, or in 500 µl/kg saline subcutaneously into the right hindlimb as previously described.[15]

Whole blood (0.15 ml) was collected into heparinised (10 U) Eppendorf tubes and centrifuged at 3500 g for 5 mins to obtain plasma. Plasma samples were mixed with 1 mL Irga Safe Plus and analysed on a Packard Tri-carb liquid scintillation counter for determination of ^{3}H content as previously described.[22] Lymph fluid collected at 1-12 hour intervals was mixed with at least 2 volumes of Irga Safe Plus and analysed as above. Rats administered methotrexate and rats bearing indwelling thoracic lymph duct cannulas were euthanized 30 h after dosing. Rats administered D-MTX(OH) were euthanized 72 h after dosing and rats administered D-MTX(OtBu), D-COOH or D-NH$_2$ were euthanized after 120 h. After termination of non-lymph cannulated rats, major organs (liver, lungs, heart, spleen, pancreas, kidneys) and lymph nodes (popliteal and inguinal nodes on the ipsilateral side to dosing and iliac nodes) were collected from non-lymph cannulated animals and analysed for ^{3}H content (see supporting information). Size exclusion chromatography (SEC) was also used to identify the radiolabelled species present in plasma and lymph samples collected from SC dendrimer dosed animals as described in the supporting information.

Size exclusion chromatography of plasma and lymph samples after SC administration of methotrexate-conjugated dendrimers in rats

Size exclusion chromatography was used to identify the radiolabelled species present in plasma and lymph samples collected from SC dosed dendrimers, with the exception of D-MTX(OH) which was undetectable in plasma following SC administration. Samples were diluted 1:1 in mobile phase where tritium counts were sufficiently high and 100-200 µl volumes injected onto a size exclusion column as previously described[20]. Chromatographic conditions were as reported previously[20] with samples eluted on a Superdex 200 column to allow better separation of the larger molecular weight (MW) species present in lymph and plasma. To identify whether the MTX-dendrimers bind to components of the plasma or lymph to form high molecular weight products, solutions of dendrimer diluted only in phosphate buffered saline (PBS) were compared to dilutions in plasma or lymph and incubation at 37°C for 1 h prior to injected onto the column.

8

Rat model of lymph-metastatic cancer

Lymphatic metastases were established in the left popliteal lymph node of syngeneic female F344 rats by injecting 1×10^5 MAT cells in 50 μl DPBS SC into the left footpad. Primary tumour growth in the footpad was evidenced initially by swelling, and later by the formation of a solid palpable mass. This led to the establishment of micrometastases in the ipsilateral popliteal lymph node within 12 days, and this was confirmed by the presence of cancer cells expressing mCherry fluorescent protein in the popliteal lymph node by laser scanning confocal fluorescence microscopy (Nikon® A1-R, Japan). Primary and secondary tumour growth, walking, rearing behaviour and body weight were monitored every 2 days. As a result of the growth of the footpad tumour eventually impacting on the ability to walk and rear, rats were euthanized 3 weeks after injection of cells.

Biodistribution of dendrimers to tumour and non-tumour burdened lymph nodes

The biodistribution of SC administered MTX and MTX-dendrimers in non-tumour burdened lymph nodes was determined as described above in male SD rats. In addition, the biodistribution of MTX and MTX-dendrimers into popliteal lymph nodes bearing palpable MAT metastases was assessed in female F344 rats after SC and IV administration. Lymph node metastases were established in the left popliteal lymph node as described above. Once the popliteal nodes reached a palpable size of approx 3 mm in diameter, rats were administered 5 mg/kg of ^{3}H-labelled MTX, D-MTX(OH), D-MTX(OtBu) or D-NH$_2$ SC (via the inner ipsilateral heel in a volume of 500 μl/kg saline) or IV (via a lateral tail vein in a volume of 500 μl saline). Rats were sacrificed 3 days later and popliteal lymph nodes were removed, weighed and analysed for ^{3}H content as previously described.[15] Statistical analysis was performed using two-way ANOVA to compare cancerous and non-cancerous nodes, dosing route and dendrimer treatment.

Confocal microscopy and & flow cytometric assessment of D-MTX(OH) distribution and cell targets in tumour-burdened lymph nodes

In order to identify the cellular targets for D-MTX(OH) within tumour-burdened lymph nodes, an additional group of rats were injected via the footpad with mCherry-expressing MAT cells that were generated according to the methods described in the supporting information. Twelve days after injection of MAT cells, rats were given 0.5 mg Atto488-labelled D-MTX(OH) SC into the heel ipsilateral to tumour growth. Rats were euthanised 3 days later and ipsilateral popliteal and inguinal lymph nodes, the iliac node and contralateral popliteal lymph nodes were removed. Nodes were initially imaged on a Caliper IVIS II fluorescence imager (Perkin Elmer) to identify the

9

drainage pattern from the SC injection site and the extent of D-MTX(OH) retention in the different nodes. Fresh ipsilateral popliteal lymph node sections (150 μm) were then cut using a vibratome and sections imaged on a glass microscope slide at 4X magnification using a laser scanning confocal microscope to visualise the regional distribution of D-MTX(OH) within the node. The remainder of the lymph nodes were dissociated via enzymatic digestion to create single cell suspensions for flow cytometry analysis according to the following procedure.

Lymph nodes were enzymatically dissociated in 2.5 ml RPMI (with RPMI containing 2.5% serum-containing, 1 mg/ml collagenase IV, 0.5 mg/mL dispase, 250 U/ml DNaseI) at 37°C for 40-60 min followed by mechanical dissociation using the gentleMACS™ dissociator (C-tube programme, Miltenyi Biotech). Cell suspensions were diluted 1:1 with PBS containing 4 mM EDTA/4% FBS and passed through a 100 μm cell strainer. Cells were pelleted at 300 x g for 5 min and resuspended in ACK Lysis buffer (Life technologies, Victoria, Australia) to remove red blood cells before being counted by a hemocytometer. Aliquots of cell suspension in FACS buffer (PBS containing 1% BSA, 2 mM EDTA) were blocked with mouse anti-rat CD32 Fc block for 5 min at 4°C and incubated with fluorescent-labelled primary antibodies against various immune cells (as below) for 30 min at room temperature. Antibodies used included PE-Cy7 labelled mouse anti-rat CD45+ to stain for all leucocytes, APC labelled mouse anti-rat CD3 to stain for T lymphocytes and PE labelled mouse anti-rat macrophage subset to stain for macrophages with PE labelled isotype control. SYTOX Blue dead cell dye was used to eliminate non-viable cells. Tumour cells were identified by mCherry expression and their failure to bind CD45 antibody. Total cell count in the lymph node cell suspensions was determined by adding a known volume of the cell suspension into BD Trucount tubes. Trucount tubes contain a fixed number of FITC-labelled beads per tube and enable a determination of the total number of cells analysed by the flow cytometer versus the total number of cells in the entire homogenised sample.

mCherry expressing cancer cells, antibody-labelled immune cells and D-MTX(OH) associated cells were detected by multi-colour fluorescence flow cytometry on a MoFlo® Astrios™ (Beckman Coulter, NSW, Australia). The following excitation lasers and bandpass filter sets (nm) were used to achieve appropriate spectral separation; 488ex, 525/50em for atto-488; 488ex, 595/50em for PE; 594ex, 620/30em for mCherry; 561ex, 790/80em for PE-Cy7; 647ex, 671/30em for APC. Single colour compensation controls were run for all samples and the data were analysed on FlowJo Software (TreeStar Inc., USA). The total D-MTX(OH) content in the supernatant and cellular fraction was also quantified by fluorescence detection on a Fluostar OPTIMA plate reader (BMG Labtech, Mornington, VIC, Australia).

10

Chemotherapeutic activity of SC and IV administered dendrimers against lymph node metastases

Popliteal metastases were induced via the injection of MAT 13762 IIIB cells into the right footpad of F344 rats as described above. On day 12 and 16 saline vehicle, MTX, D-MTX(OH) or D-MTX(OtBu) were administered at a dose of 5 mg/kg MTX equivalents SC into the inner right hindlimb just above the heel in a volume of 500 μl/kg body weight, or IV via a lateral tail vein in a volume of 500 μl. Rats were sacrificed on day 20 and popliteal lymph nodes removed and weighed as an indicator of popliteal tumour burden. To confirm the presence of significant tumour burden after 20 days, lymph nodes from 2 saline dosed rats were fixed in 10% formalin and assessed histologically as described in the supporting information. Histological evaluation of the lymph nodes showed that approximately 95% of the node mass was attributed to tumour tissue and that cancer cells were approximately 4 times larger than lymphocytes (supporting information, Figure S1). An additional set of popliteal lymph nodes from saline control and SC dosed D-MTX(OH) rats were processed for flow cytometry analysis to quantify the number of tumour cells relative to immune cells. Detection of cell types was as previously described[23] with the total cell number determined by the addition of a known volume of cell suspension to BD Trucount tubes that contain a known number of FITC-labelled fluorescent beads.

Calculation of pharmacokinetic parameters and statistics

Plasma concentrations were normalised to 5 mg/kg based on the body weight of rats prior to dosing and are expressed as ng/ml. Pharmacokinetic parameters were calculated from individual plasma concentration versus time profiles as previously described[15] and values are reported as mean ± SD (n=3-4). Pharmacokinetic data for D-MTX(OH), D-MTX(OtBu) and $D-NH_2$ after IV administration to SD rats were reported previously[20, 24], and were used here to enable the calculation of bioavailability after SC administration. Data from SC lymph-cannulated rats enabled determination of the proportion of the dose of dendrimer or MTX that was absorbed via the lymph versus via the blood after SC administration.

Maximum plasma concentrations (C_{max}) and time to maximum concentration (T_{max}) were taken directly from the plasma concentration time curves. Linear regression of the terminal post-distributive portion of the plasma concentration-time curve was used to determine the plasma elimination rate constant (K_{el}). The area under the plasma concentration-time curves (AUC^{0-last}) was calculated using the linear trapezoid rule to the last plasma concentration determined (C_{last}). The extrapolated terminal AUC ($AUC^{last-\infty}$) was calculated from C_{last}/K_{el} and was added to the AUC^{0-last} to give total area ($AUC^{0-\infty}$). Plasma clearance (Cl) was calculated from the dose/$AUC^{0-\infty}$ for the IV control group. The bioavailability (percent of the dose absorbed and transported intact into the systemic blood) in the SC control group (F) was calculated by dividing the AUC_{SC} by AUC_{IV} and

11

multiplying by 100. In SC lymph cannulated animals the percent bioavailability in blood (F_{blood}) could not be determined for dendrimer dosed animals, since no distinct elimination phase was evident by 30 h post dose.

The plasma concentration-time profiles for MTX, D-MTX(OtBu) and D-NH$_2$ after SC administration in lymph-cannulated and non cannulated rats were compared via 2-way ANOVA with Bonferroni's test for least significant differences at each time point. An unpaired T-test was used to compare the C_{max} and T_{max} between lymph cannulated and uncannulated rats. The anticancer activity in rats administered MTX, D-MTX(OtBu) or D-MTX(OH) via the IV or SC routes was compared to rats administered SC saline vehicle via 1 way AVOVA with a Tukey's post test for least significant differences. Significance was determined as $p<0.05$.

Results:

Lymphatic transport and biodistribution of dendrimers and methotrexate

The dendrimer where 50% of surface groups were PEGylated and 50% left underivatised, (D-NH$_2$) was absorbed slowly after SC administration into the inner left heel of rats, reaching peak plasma concentrations of approximately 12 μg/ml after 1 day (Figure 2A). Approximately 76% of the SC dose was absorbed (Table 1). The organ biodistribution profiles after IV and SC administration are shown in Figure 3. The patterns of organ disposition for D-NH$_2$ were similar in IV and SC dosed rats and the levels of dendrimer in the organs of SC dosed rats was approximately 25-50% lower than that in the IV group, presumably reflecting incomplete absorption. The similar biodistribution patterns after SC and IV administration are consistent with the fact that the major ^{3}H species in plasma and lymph (with the exception of liberated monomeric ^{3}H-lysine at later time points) was intact dendrimer (SEC profiles in Figures S2 & S3, supporting information). The biodistribution pattern after SC administration therefore matched the biodistribution pattern of the intact dendrimer after IV administration.

After SC administration to lymph cannulated animals, the fraction of the dose recovered in the lymph up to 30 h post dose for D-NH$_2$ was 19% (Figure 4, Table 1). As a result, the plasma concentration-time profiles showed lower levels of D-NH$_2$ in the plasma of thoracic lymph duct cannulated rats when compared to rats with an intact lymph-blood circuit (Figure 2A). C_{max} in lymph cannulated rats was significantly lower (4.8 vs 11.9 μg/ml) than that in SC control rats.

D-COOH had a similar IV pharmacokinetic profile to that of D-NH$_2$, despite the presence of anionic rather than cationic charge on 50% of available surface groups (Figure 2B). The SC bioavailability of D-COOH was slightly lower than D-NH$_2$ (59% when compared to 76%, Table

1). The organ deposition of D-COOH was similar between IV and SC dosed rats, despite the lower SC bioavailability (Figure 3). SEC profiles revealed some breakdown of the dendrimer in plasma samples 24-96 hours after SC administration (Figure S2, supporting information). No evidence of high molecular weight species was seen after incubation with plasma or after SC dosing, suggesting that D-COOH does not bind to plasma proteins. After SC administration of D-COOH to lymph cannulated animals approximately 14% of the injected ^{3}H dose was recovered in lymph as intact dendrimer over 30 h and this did not differ significantly when compared to the lymphatic recovery of D-NH$_2$ (Figure 4, Table 1; Figure S3, supporting information). Consistent with the lymphatic transport data, the plasma concentration-time profiles of D-COOH in lymph cannulated animals were lower than that in non-lymph cannulated rats (Figure 2B), as seen for D-NH$_2$.

D-MTX(OtBu) was absorbed at a similar rate to D-NH$_2$ and D-COOH, reaching peak plasma concentrations of approximately 11.7 μg/ml after 1 day (Figure 2B, Table 1). The fraction of the dose absorbed, however, was lower (47%). The pattern of organ biodistribution for D-MTX(OtBu) after SC administration was again similar to that after IV administration (Figure 3). SEC profiles revealed that ^{3}H-D-MTX(OtBu) was present in plasma and lymph mainly as high molecular weight species that eluted over 18-34 mins (Figure S2 & S3, supporting information). This was also the case after intravenous administration for D-MTX(OtBu) and suggests that D-MTX(OtBu) exists in biological fluids as high molecular weight species, for example aggregates or opsonised species[20]. The absorption of D-MTX(OtBu) into the lymph after SC administration to lymph cannulated animals was significant (24% of the SC dose of D-MTX(OtBu) was absorbed via the lymph over 30 h) resulting in considerably lower plasma levels in lymph cannulated animals when compared to control (lymph intact) animals (Figure 4).

In contrast to the other dendrimers, plasma levels of D-MTX(OH) were below the level of quantification at all times after SC administration. This likely reflected both poor absorption and rapid plasma clearance of D-MTX(OH). The absolute fraction of D-MTX(OH) absorbed could therefore not be calculated based on the plasma concentration-time profiles. The organ biodistribution profiles suggested that approximately 10% of the dose gained access to the systemic circulation over 3 days since approximately 10% of the dose was recovered in the liver and spleen (Figure 3). Note that almost the entire IV dose of D-MTX(OH) was recovered in the liver and spleen after 3 days providing support for the use of this quantity as an indicator of absorption in SC dosed animals.[20] For comparison, the plasma profiles for each dendrimer construct and MTX after IV administration are shown in Figure S4 (supporting information).

The proportion of an SC dose of D-MTX(OH) that was recovered in thoracic lymph over 30 h was also lower (5%) than the other dendrimers, however, in light of the low overall absorption a large proportion of the absorbed dose was lymphatically transported (Table 1, Figure 4). The SEC

13

profile of D-MTX(OH) in lymph also showed the presence of high molecular weight material (supporting information, Figure S3). Incubation of D-MTX(OH) with fresh lymph did not result in the formation of the same high molecular weight species, suggesting that the ^{3}H-labelled D-MTX(OH) was absorbed in this form rather than being assembled in lymph. It is not known whether this high molecular weight material was formed via interaction with soluble proteins in the interstitium or whether it represented dendrimer aggregates.

The fraction of the solution formulation of MTX that was absorbed from an SC injection site was 74% (consistent with previously reported SC pharmacokinetics in rats and humans[25]). In contrast to the dendrimer-based formulations of MTX, absorption occurred almost exclusively via the blood, with only 2% of the dose recovered in thoracic duct lymph over 30 h.

Biodistribution of dendrimers and MTX in non-cancerous and tumour burdened lymph nodes

Previous studies have shown that D-MTX(OH) is rapidly cleared from the systemic circulation by the organs of the MPS[20], limiting tumour access from the blood via EPR. This property, however, might be expected to promote capture by macrophages in lymph nodes after SC administration, promoting targeting to sites of lymph metastatic spread. In contrast, D-MTX(OtBu) more effectively evades MPS clearance and has increased potential to gain access to lymph nodes and lymph resident tumours via EPR. MTX(OtBu) also has the potential to access the lymph (and lymph nodes) directly from the injection site.

The biodistribution of dendrimers and MTX in non-cancerous and tumour burdened lymph nodes were therefore examined after IV and SC administration (Figure 5A). SC administration of D-NH$_2$, D-COOH or D-MTX(OtBu) led to the retention of approximately 1.3 to 2.6% injected dose/g in non-tumour bearing primary (popliteal) and secondary (iliac and inguinal) lymph nodes. Retention of dendrimers in tumour burdened popliteal nodes was ~2-3 fold higher (4-7% injected dose/g). D-COOH retention in tumour-burdened nodes was not examined since retention in non-tumour burdened lymph nodes was similar to that of D-NH$_2$. In contrast, the retention of D-MTX(OH) in non-tumour burdened and tumour-burdened lymph nodes was significantly higher (up to 10 fold) than that of D-NH$_2$, D-COOH or D-MTX(OtBu), with approximately 28 to 36% of the injected dose retained per gram of lymph node tissue after SC administration, in spite of the relatively low overall absorption. This value is also probably a conservative estimate of uptake into the popliteal lymph node alone (rather than pooled lymph nodes), since ex vivo fluorescence imaging of lymph nodes after injection of atto488-labelled D-MTX(OH) showed higher retention in the popliteal lymph node when compared to other nodes (Figure 5B).

14

After IV administration of D-NH$_2$, D-MTX(OtBu) or D-MTX(OH) to rats bearing popliteal lymph node metastases, the retention of the dose in the tumour burdened lymph nodes was only 1 to 2%/g, suggesting that SC administration improved exposure to downstream lymph nodes. The retention of MTX in lymph nodes after IV or SC dosing was less than 0.3%/g (not shown), suggesting limited lymph node retention for the solution formulation of the drug.

The mechanisms by which PEGylated dendrimers target tumours and macrophages in MPS organs after IV administration is well established. The mechanism by which PEGylated dendrimers (in particular D-MTX(OH)) target lymph nodes downstream from an SC injection site or lymph node resident metastases is less clear. We therefore sought to examine the patterns of lymph node and lymph node metastasis disposition after SC administration of D-MTX(OtBu) and D-MTX(OH).

To determine whether D-MTX(OH) was retained in lymph nodes as a result of physical filtration or via electrostatic interactions with, or internalisation into cells, initial studies examined whether the dendrimer was associated with the supernatant or cell pellet following lymph node homogenisation. This could not be determined for D-MTX(OtBu) since lymph node retention was too low to accurately quantify the ^{3}H label in both the cell pellet and supernatant). For D-MTX(OH) approximately 96% of the dendrimer in the node 3 days after SC administration was associated with the supernatant, and only 4% with the cell pellet. In addition, visualisation of the localisation of Atto-488 labelled D-MTX(OH) within whole lymph nodes via confocal fluorescence microscopy indicated that the dendrimer was distributed throughout the lymph node (Figure 6A). As expected, no fluorescence was detected in the lymph nodes of D-MTX(OtBu) dosed rats (not shown). This suggests that in non-tumour bearing lymph nodes, D-MTX(OH) is retained primarily via physical filtration, rather than cell association.

A recent study by Baker and colleagues has suggested that MTX-conjugated dendrimers may be internalised into macrophages and cancer cells that overexpress beta and alpha folate receptors respectively [26, 27]. Flow cytometry was therefore used to determine dendrimer (Atto-488 labelled D-MTX(OH)) association with macrophages and MAT cancer cells in tumour bearing lymph nodes 3 days after SC administration. Approximately 20% of MAT 13762 IIIB cells and macrophages in lymph nodes were positive for Atto488-labelled D-MTX(OH). In contrast less than 3% of total leucocytes and T-lymphocytes were positive for dendrimer (Figure 6B). Confocal fluorescence microscopy of a section of lymph node tissue also showed that the majority of the Atto label (and therefore the dendrimer) was located in the lymph node parenchyma, rather than within metastatic foci (Figure 6C), suggesting that D-MTX(OH) targeted macrophages and cancer cells surrounding areas of lymph fluid flow rather than in metastatic foci.

Anticancer activity against lymph node metastases of rat breast carcinoma

15

The anticancer activity of MTX and the MTX-conjugated dendrimers was examined against popliteal metastases derived from a primary MAT carcinoma. After the injection of cancer cells into the footpad of syngeneic rats, popliteal lymph nodes increased in size from approximately 10 mg at the time of first drug dose to approximately 100 mg at day 20 after initiation of the primary tumour.

To identify whether localised (i.e. SC) administration of the lymph node-targeted D-MTX(OH) provided therapeutic advantage when compared to IV administration of drug or dendrimer, or SC administration of non-lymph node targeted D-MTX(OtBu) or methotrexate, anticancer activity was assessed for all MTX preparations after IV and SC administration. SC or IV administration of MTX at 5 mg/kg twice over 8 days failed to significantly reduce lymph node tumour burden (Figure 7A). In contrast, SC and IV administration of D-MTX(OtBu) and D-MTX(OH) significantly reduced tumour burden in the lymph node by approximately 30 to 50%. Figure 7A shows a trend towards increased anticancer activity for D-MTX(OtBu) after IV administration when compared to SC administration (suggesting anticancer activity mainly via enhanced permeation and retention of the dendrimer into the microtumour mass). In contrast, D-MTX(OH) was equally effective after SC and IV administration.

To confirm that the reduction in popliteal lymph node mass was due to the chemotherapeutic activity of methotrexate, FACS analysis of cell populations in the lymph nodes of rats treated with saline control or SC D-MTX(OH) revealed that the reduction in popliteal mass was a result of reduced numbers of MAT cancer cells and macrophages that typically increase in number with tumour growth[28] (Figure 7B). In contrast, the number of leukocytes remained unchanged between control and D-MTX(OH) dosed rats.

Discussion:

Metastatic spread of cancer is the major cause of cancer-related death. Surgical intervention combined with chemo- and radiation therapies can eradicate much of the tumour burden, however, this approach is often not sufficient to remove all cancer cells, including cancer stem cells and metastatic nodules.[29, 30] This can lead to the regrowth of drug resistant tumours that become increasingly difficult to treat. Dose related toxicity induced via the systemic administration of chemotherapeutic drugs also often prohibits the use of escalating doses, and may preclude the use of certain combinations of macromolecular and small molecule therapeutics.[31-33] In light of these complications, there is increasing interest in the localised administration of chemotherapeutics. Localised administration has the potential to provide high drug concentrations at the site of tumour resection and to promote the killing of tumour cells that persist post surgery (such as at the site of glioma removal, where tumour resection is often incomplete [34]). Local administration may also

16

promote uptake into draining lymphatics, thereby enhancing the elimination of disseminating cancer cells in sentinel lymph nodes. In the current study, we have examined the potential utility of localised administration of drug-conjugated dendrimers as a means of targeting sites of lymph-metastatic spread, since dendrimers have previously been shown to preferentially access the lymphatics after SC administration when compared with small molecule drugs or PEGylated liposomes.[10]

Consistent with previous studies of similarly sized doxorubicin-conjugated dendrimers[10] the PEGylated and MTX-conjugated systems explored here were incompletely absorbed after SC administration. However, in all cases, a significant proportion of the absorbed dose was taken up into the lymphatics from the injection site, and retention in downstream lymph nodes was significantly higher than that observed after administration of a solution formulation of methotrexate. Although lymphatic targeting was evident with all the dendrimer-based systems, notable differences were evident across the three constructs examined. The non drug-conjugated dendrimer core (D-NH$_2$) (that comprised a surface with 50% PEG and 50% underivatised amine groups) was relatively well absorbed (76% bioavailability) and 19% of the dose was recovered in the draining lymphatics up to 30 hr post injection. This was slightly lower than that seen previously for a similarly sized, but fully PEGylated (and uncharged), dendrimer where absorption was essentially complete and the proportion of the dose recovered in the lymph was 30% over 30 h.[15] The incomplete absorption of D-NH$_2$ observed here was likely a function of the interaction of the partial positive charge on the dendrimer with the interstitial matrix.[35] Conjugation of the surface amine groups of D-NH$_2$ with either GILGVP-glutamic acid (to give a non drug-conjugated anionic control dendrimer, D-COOH), or O-*t*-butylated or underivatised MTX via the same hexapeptide linker to form D-MTX(OtBu) or D-MTX(OH) respectively resulted in further decreases in absorption. In the case of D-MTX(OtBu) and D-COOH the reduction was moderate and approximately 50% of the dose was absorbed and 25% of the administered dose was transported into the lymph for D-MTX(OtBu) and 14% for D-COOH. In contrast, absorption of D-MTX(OH) was very low (approximately 10%). This may have resulted from interaction of the polyanionic charge associated with the uncapped carboxylic acid of MTX with cationic charge in the interstitium[15], or via interaction with folate or folate-related receptors on cells within the interstitium. A complete explanation for this behaviour is not evident at this time although the relatively robust absorption and lymphatic transport of D-COOH suggests that a simple charge-charge interaction in unlikely to completely explain the differential behaviour of D-MTX(OH).

Although the SC absorption of D-MTX(OH) was low, a significant proportion of the absorbed dose was recovered in lymph, and a very large proportion of the absorbed dose was retained in the draining lymph nodes. Indeed, after SC administration of D-MTX(OH), recovery in

17

the draining lymph nodes was approximately 10 fold higher than that observed for D-MTX(OtBu), D-COOH or D-NH$_2$, in spite of the fact that absorption from the injection site was approximately 5 fold lower. When comparing SC and IV administration, recovery in the lymph nodes was approximately 2-fold higher after SC administration for most dendrimers. For D-MTX(OH), however, where lymph node recovery was high after SC administration, the difference was more profound and lymph node recovery was increased approximately 20 fold after SC administration. Lymph node recovery was very low after both SC and IV administration of the MTX solution.

In comparison to MTX alone, D-MTX(OtBu) and D-MTX(OH) therefore provided markedly different disposition profiles. D-MTX(OtBu) resulted in prolonged plasma exposure after SC and IV dosing, enhanced lymphatic exposure and enhanced lymph node retention after IV (3-5 fold) and SC (10-20 fold) administration when compared to MTX. In contrast, D-MTX(OH) resulted in limited plasma exposure after IV administration and very low plasma exposure after SC administration. Absolute lymphatic recovery after SC administration was higher than that of MTX, but approximately 4 fold lower than that of D-MTX(OtBu). After IV administration lymph node recovery was similar to that of D-MTX(OtBu) and therefore moderately (approximately 5 fold) higher that that after IV administration of MTX. Notably, however, after SC administration, lymph node retention for D-MTX(OH) was very high (approximately 100 fold higher than for MTX).

Subsequent studies therefore sought to evaluate the impact of the differing disposition profiles of the MTX dendrimers on chemotherapeutic activity in a syngeneic model of metastatic cancer. In all cases, administration of dendrimer-MTX resulted in more effective inhibition of the growth of lymph node metastases when compared to MTX alone, consistent with previous studies in a non-metastatic xenograft model.[20] Surprisingly, however, in spite of the increase in lymph node recovery of both dendrimers after SC administration when compared to IV administration, the reduction in lymph node mass was no higher after SC administration, and in fact for D-MTX(OtBu) activity was moderately (although insignificantly) higher after IV administration. The data were particularly surprising for D-MTX(OH) where lymph node recovery was very high, but where, activity was not improved.

In an attempt to better understand the high recovery of D-MTX(OH) in lymph nodes and potentially to provide an explanation for the disconnect between lymph node disposition and activity against lymph node resident metastatic cancer, a series of experiments were undertaken to evaluate the patterns of dendrimer disposition within lymph nodes and tumour burdened lymph nodes. These data suggested that whilst recovery of D-MTX(OH) in lymph nodes was high, the dendrimer was present in large part (>90%) in the supernatant of lymph node homogenate, and was not internalised into lymph node resident cells. Confocal fluorescence microscopy of tumour bearing lymph nodes after SC administration of Atto-488 labelled D-MTX(OH) also showed that

18

the majority of the retained dose was located within the lymph node parenchyma and not within the metastatic foci. As such only limited colocalisation of Atto-488 labelled D-MTX(OH) with mCherry labelled tumour cells (and more importantly, the centre of the tumour mass) was apparent. FACS analysis of a mixed population of cells obtained from a lymph node with metastatic invasion also suggested that although cellular interaction of D-MTX(OH) with MAT13762 IIIB cells and macrophages was higher than that of lymph node resident leucocytes (consistent with the recent suggestion that MTX-conjugated dendrimers may be internalised into macrophages and cancer cells that overexpress beta and alpha folate receptors respectively [26, 27]), the degree of cellular association was relatively low (~20% of tumour cells and macrophages were positive for the fluorescently labelled dendrimer). It seems likely therefore that whilst macrophages play a role in the retention of D-MTX(OH) in MPS organs after IV administration, after SC administration, retention in the lymph nodes appears to be driven largely via a physical interaction with the lymph node parenchyma, with a more minor component associated with cellular/macrophage targeting. The lack of significant colocalisation of D-MTX(OH) with metastatic foci in lymph nodes is also consistent with the poor correlation between high levels of lymph node retention of D-MTX(OH) and activity against metastatic tumours. It seems likely therefore that the high level of lymph node retention of D-MTX(OH) after SC administration was not productive with respect to tumour killing, since the dendrimer was not distributed to the centre of metastatic nodules. This likely precluded effective release of MTX from D-MTX(OH) via extracellular matrix metalloprotease 2 (MMP2), since sequestration in the lymph node occurred at a site distant from the tumour and therefore at a site where MMP levels were expected to be low, leading to incomplete drug release. It is also possible that MMP2 mediated drug cleavage within the lymph node may be saturated at only low levels of dendrimer. This is consistent with the similar anticancer activity of SC administered D-MTX(OH) and D-MTX(OtBu), despite significant differences in lymph node retention. It might be expected, therefore, that by employing a more labile chemical linker or a tumour that expresses higher levels of MMP2, MTX liberation may be more efficient. Under these circumstances, released MTX may be able to convect through the lymph node, resulting in increased anticancer activity, even in the absence of absolute colocalisation of the dendrimer with metastatic foci.

In summary, the results of this study show differential patterns of lymphatic uptake and lymph node disposition for PEGylated MTX dendrimers after SC and IV administration that were dependent upon the chemical properties of the conjugated drug. Conjugation of MTX to the surface of the dendrimer significantly reduced absorption from SC injection sites, but also resulted in very efficient targeting to draining lymph nodes. These effects were attenuated by OtBu capping of the MTX carboxylic acid, which resulted in improved absorption and enhanced long circulation properties, but less effective lymph node retention. Both MTX-conjugated dendrimers resulted in

19

improved activity against lymph node resident metastases (when compared to MTX alone), but correlation of lymph node retention with anticancer activity was poor and indeed activity was similar after IV administration and SC administration, whereas lymph node deposition was far more effective after SC administration. In the case of D-MTX(OH) (which was poorly absorbed after SC administration, but highly retained in lymph nodes) this likely reflected dendrimer sequestration within areas of the lymph node that were not directly associated with metastatic invasion, despite efficient retention by cancer cells and lymph node resident macrophages. This in turn might be expected to either reduce drug liberation from the dendrimer (since the releasing technology relies on the presence of MMPs) or provide a diffusional distance between the site of drug release and drug activity that is too great to allow useful activity. Subsequent studies will attempt to better harness the lymph node targeting capabilities of PEGylated dendrimers and explore the means by which drug disposition into metastatic sites within lymph node tumours can be enhanced.

Supporting Information:

Supporting information shows the synthetic methods and characterisation data for D-COOH, details of the histological evaluation of tumour-burdened lymph nodes, size exclusion chromatography data for ^{3}H-species present in plasma and lymph, a comparison between the IV pharmacokinetics of all the constructs evaluated in this study, the method of preparation of mCherry-labelled cells, and the in vitro cytotoxicity data for the MTX-dendrimers. This information is available free of charge via the Internet at http://pubs.acs.org/.

20

References:

1.   Wong, D. J.; Liu, H.; Ridky, T. W.; Cassarino, D.; Segal, E.; Chang, H. Y. Module map of stem cell genes guides creation of epithelial cancer stem cells. *Cell Stem Cell* **2008,** *2*, 333-44.

2.   Passaro, A.; Trenta, P.; Conte, D.; Campenni, G.; De Benedetto, A.; Cortesi, E. The impact of chemotherapy on the lymphatic system in thoracic oncology. *Thoracic Surg Clinic* **2012,** *22*, 243-9.

3.   Glechner, A.; Wockel, A.; Gartlehner, G.; Thaler, K.; Strobelberger, M.; Griebler, U.; Kreienberg, R.   Sentinel lymph node dissection only versus complete axillary lymph node dissection in early invasive breast cancer: a systematic review and meta-analysis. *Eur J Cancer* **2013,** *49*, 812-25.

4.   McCarthy, W. H.; Shaw, H. M.; Cascinelli, N.; Santinami, M.; Belli, F. Elective lymph node dissection for melanoma: two perspectives. *World J Surg* **1992,** *16*, 203-13.

5.   Fife, K.; Thompson, J. F. Lymph-node metastases in patients with melanoma: what is the optimum management? *Lancet Oncology* **2001,** *2*, 614-21.

6.   Capitanio, U.; Becker, F.; Blute, M. L.; Mulders, P.; Patard, J. J.; Russo, P.; Studer, U. E.; Van Poppel, H. Lymph node dissection in renal cell carcinoma. *Eur Urology* **2011,** *60*, 1212-20.

7.   Cockerell, C. J.; Lyons, J. H.   Elective Regional Lymph-Node Dissection in Cutaneous Melanoma. *J Dermatol Treat* **1995,** *6*, 127-134.

8.   Psaila, B.; Kaplan, R. N.; Port, E. R.; Lyden, D.   Priming the 'soil' for breast cancer metastasis: the pre-metastatic niche. *Breast Dis* **2006,** *26*, 65-74.

9.   Kaplan, R. N.; Psaila, B.; Lyden, D. Bone marrow cells in the 'pre-metastatic niche': within bone and beyond. *Cancer Met Rev* **2006,** *25*, 521-9.

10.   Ryan, G. M.; Kaminskas, L. M.; Bulitta, J. B.; McIntosh, M. P.; Owen, D. J.; Porter, C. J. H. PEGylated polylysine dendrimers increase lymphatic exposure to doxorubicin when compared to PEGylated liposomal and solution formulations of doxorubicin. *J Control Release* **2013,** *172*, 128-136.

11.   Hofheinz, R. D.; Gnad-Vogt, S. U.; Beyer, U.; Hochhaus, A. Liposomal encapsulated anti-cancer drugs. *Anti-Cancer Drugs* **2005,** *16*, 691-707.

12.   Stinchcombe, T. E. Nanoparticle albumin-bound paclitaxel: a novel Cremphor-EL-free formulation of paclitaxel. *Nanomedicine (Lond)* **2007,** *2*, 415-23.

13.   Nowotnik, D. P.; Cvitkovic, E.   ProLindac (AP5346): a review of the development of an HPMA DACH platinum Polymer Therapeutic. *Adv Drug Deliv Rev* **2009,** *61*, 1214-9.

14.   Kaminskas, L. M.; Ascher, D. B.; McLeod, V. M.; Herold, M. J.; Le, C. P.; Sloan, E. K.; Porter, C. J. H. PEGylation of interferon alpha2 improves lymphatic exposure after subcutaneous

21

and intravenous administration and improves antitumour efficacy against lymphatic breast cancer metastases. *J Control Release* **2013,** *168*, 200-208.

15.   Kaminskas, L. M.; Kota, J.; McLeod, V. M.; Kelly, B. D.; Karellas, P.; Porter, C. J. H. PEGylation of polylysine dendrimers improves absorption and lymphatic targeting following SC administration in rats. *J Control Release* **2009,** *140*, 108-16.

16.   Shao, X.; Liu, Q.; Zhang, C.; Zheng, X.; Chen, J.; Zha, Y.; Qian, Y.; Zhang, X.; Zhang, Q.; Jiang, X.   Concanavalin A-conjugated poly(ethylene glycol)-poly(lactic acid) nanoparticles for intranasal drug delivery to the cervical lymph nodes. *J Microencaps* **2013,** *30,* 780-86

17.   Gunaseelan, S.; Gunaseelan, K.; Deshmukh, M.; Zhang, X. P.; Sinko, P. J.   Surface modifications of nanocarriers for effective intracellular delivery of anti-HIV drugs. *Adv Drug Deliver Rev* **2010,** *62*, 518-531.

18.   Hieu, V. Q.; Yoo, M. K.; Jeong, H. J.; Lee, H. J.; Muthiah, M.; Rhee, J. H.; Lee, J. H.; Cho, C. S.; Jeong, Y. Y.; Park, I. K.   Targeted delivery of mannan-coated superparamagnetic iron oxide nanoparticles to antigen-presenting cells for magnetic resonance-based diagnosis of metastatic lymph nodes in vivo. *Acta Biomater* **2011,** *7*, 3935-3945.

19.   Bagby, T. R.; Duan, S. F.; Cai, S.; Yang, Q. H.; Thati, S.; Berkland, C.; Aires, D. J.; Forrest, M. L.   Lymphatic trafficking kinetics and near-infrared imaging using star polymer architectures with controlled anionic character. *Eur J Pharm Sci* **2012,** *47*, 287-294.

20.   Kaminskas, L. M.; Kelly, B. D.; McLeod, V. M.; Sberna, G.; Boyd, B. J.; Owen, D. J.; Porter, C. J. H.   Capping methotrexate alpha-carboxyl groups enhances systemic exposure and retains the cytotoxicity of drug conjugated PEGylated polylysine dendrimers. *Mol Pharmaceutics* **2011,** *8*, 338-49.

21.   Kaminskas, L. M.; Kelly, B. D.; McLeod, V. M.; Sberna, G.; Owen, D. J.; Boyd, B. J.; Porter, C. J. H.   Characterisation and tumour targeting of PEGylated polylysine dendrimers bearing doxorubicin via a pH labile linker. *J Control Release* **2011,** *152*, 241-8.

22.   Boyd, B. J.; Kaminskas, L. M.; Karellas, P.; Krippner, G.; Lessene, R.; Porter, C. J. H. Cationic poly-L-lysine dendrimers: pharmacokinetics, biodistribution, and evidence for metabolism and bioresorption after intravenous administration to rats. *Mol Pharmaceutics* **2006,** *3*, 614-27.

23.   Trevaskis, N. L.; Charman, W. N.; Porter, C. J. H.   Targeted drug delivery to lymphocytes: a route to site-specific immunomodulation? *Mol Pharmaceutics* **2010,** *7*, 2297-309.

24.   Kaminskas, L. M.; McLeod, V. M.; Kelly, B. D.; Cullinane, C.; Sberna, G.; Williamson, M.; Boyd, B. J.; Owen, D. J.; Porter, C. J. H.   Doxorubicin-conjugated PEGylated dendrimers show similar tumoricidal activity but lower systemic toxicity when compared to PEGylated liposome and solution formulations in mouse and rat tumor models. *Mol Pharmaceutics* **2012,** *9*, 422-32.

22

25. Grim, J.; Chladek, J.; Martinkova, J. Pharmacokinetics and pharmacodynamics of methotrexate in non-neoplastic diseases. *Clin Pharmacokinet* **2003,** *42*, 139-51.

26. Thomas, T. P.; Goonewardena, S. N.; Majoros, I. J.; Kotlyar, A.; Cao, Z.; Leroueil, P. R.; Baker, J. R., Jr. Folate-targeted nanoparticles show efficacy in the treatment of inflammatory arthritis. *Arthritis Rheumatism* **2011,** *63*, 2671-80.

27. Thomas, T. P.; Huang, B.; Choi, S. K.; Silpe, J. E.; Kotlyar, A.; Desai, A. M.; Zong, H.; Gam, J.; Joice, M.; Baker, J. R., Jr. Polyvalent dendrimer-methotrexate as a folate receptor-targeted cancer therapeutic. *Mol Pharmaceutics* **2012,** *9*, 2669-76.

28. Pollard, J. W. Tumour-educated macrophages promote tumour progression and metastasis. *Nature Rev Cancer* **2004,** *4*, 71-8.

29. Chua, Y. J.; Steer, C.; Yip, D. Recent advances in management of small-cell lung cancer. *Cancer Treat Rev* **2004,** *30*, 521-43.

30. Ning, X.; Shu, J.; Du, Y.; Ben, Q.; Li, Z. Therapeutic strategies targeting cancer stem cells. *Cancer Biol Ther* **2013,** *14*, 295-303.

31. Friedman, A.A; Flaherty, K.T. Scratching the combinatorial drug landscape surface. *Pigment Cell Melanoma Res* **2013**. *26*, 297-99.

32. Carey, M. S.; Gawlik, C.; Fung-Kee-Fung, M.; Chambers, A.; Oliver, T. Systematic review of systemic therapy for advanced or recurrent endometrial cancer. *Gynecol Oncol* **2006,** *101*, 158-67.

33. Slamon, D. J.; Leyland-Jones, B.; Shak, S.; Fuchs, H.; Paton, V.; Bajamonde, A.; Fleming, T.; Eiermann, W.; Wolter, J.; Pegram, M.; Baselga, J.; Norton, L. Use of chemotherapy plus a monoclonal antibody against HER2 for metastatic breast cancer that overexpresses HER2. *New Eng J Med* **2001,** *344*, 783-92.

34. Preusser, M.; Haberler, C.; Hainfellner, J. A. Malignant glioma: neuropathology and neurobiology. *Wien Med Wochenschr* **2006,** *156*, 332-7.

35. Kaminskas, L. M.; Wu, Z.; Barlow, N.; Krippner, G. Y.; Boyd, B. J.; Porter, C. J. H. Partly-PEGylated Poly-L-lysine dendrimers have reduced plasma stability and circulation times compared with fully PEGylated dendrimers. *J Pharm Sci* **2009,** *98*, 3871-5.
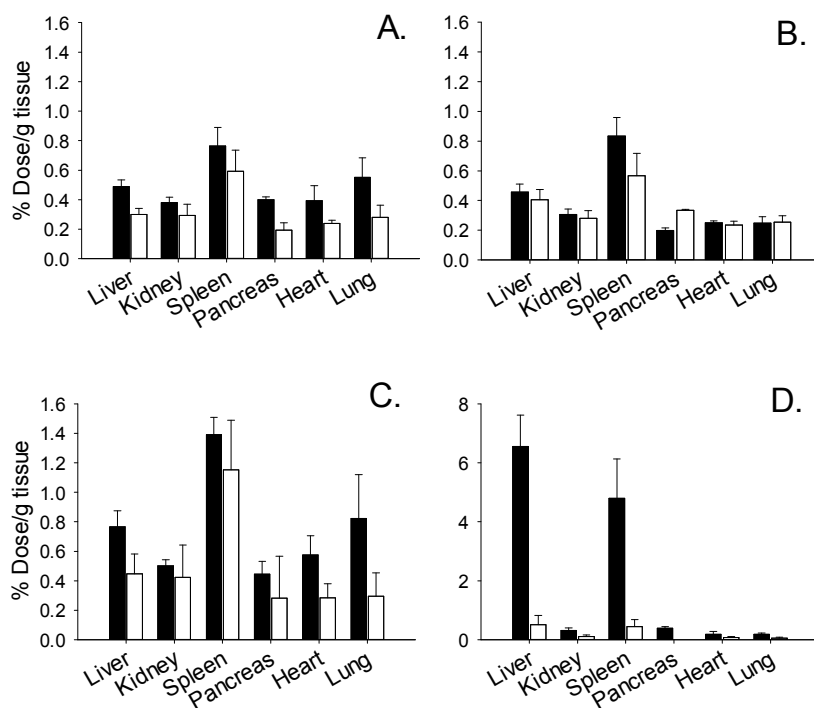
Figures:
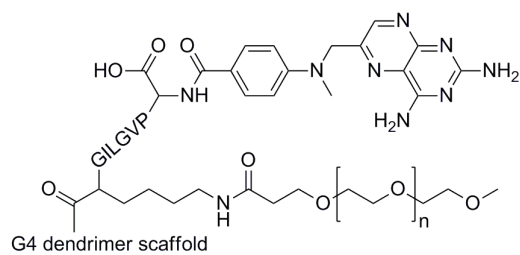
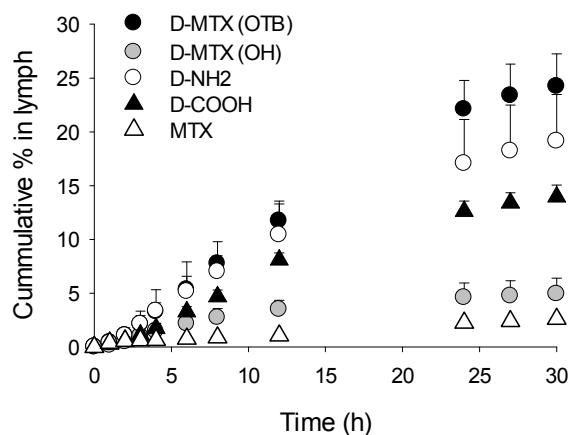**D-MTX(OH)**
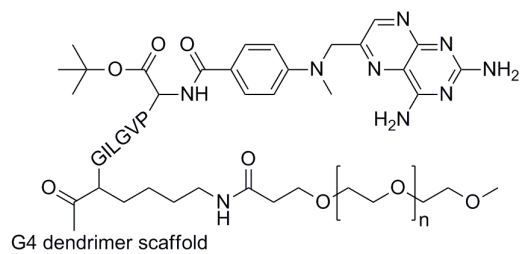
D-MTX(OtBu)

Figure 1. Structure of G5 methotrexate-conjugated dendrimers - D-MTX(OH) and D-MTX(OtBu). The surface comprised 32 lysine residues conjugated with PEG_{1100} at the ε-amino group and GILGVP-MTX (α-carboxyl capped or uncapped) at α-amino groups. The constructs have been previously described and characterized.[20]

24
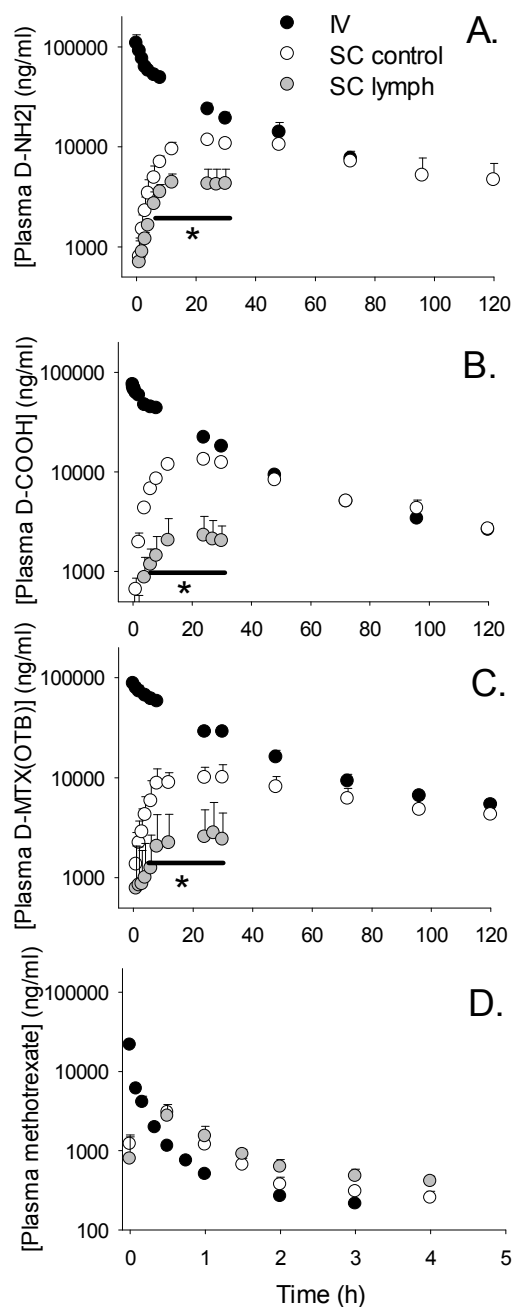
Figure 2. Plasma concentration-time profiles of D-NH$_2$ (Panel A), D-COOH (Panel B), D-MTX(OtBu) (Panel C) and MTX (Panel D) after IV and SC administration at 5 mg/kg to rats. Closed symbols represent IV plasma profiles, open symbols represent control SC plasma profiles and grey symbols represent SC plasma profiles in thoracic lymph duct cannulated animals. Data represents mean ± s.d. (n=3-5). * represents significantly lower plasma concentrations in lymph cannulated rats when compared to SC control rats at each time point indicated by the bar.

25

Figure 3: Organ biodistribution of D-NH$_2$ (Panel A, 120 h), D-COOH (Panel B, 120 h), D-MTX(OtBu) (Panel C, 120 h) and D-MTX(OH) (Panel D, 72 h) after IV (solid bars) or SC (open bars) administration of 5 mg/kg dendrimer to rats. Data represents mean ± s.d. (n=3).

Figure 4. Cumulative recovery of D-MTX(OtBu) (closed circles), D-MTX(OH) (grey circles), D-NH$_2$ (open circles), D-COOH (closed triangles) or methotrexate (open triangles) in thoracic lymph after SC administration into the left inner heel of rats. Data represents mean ± s.d. (n=3-5).
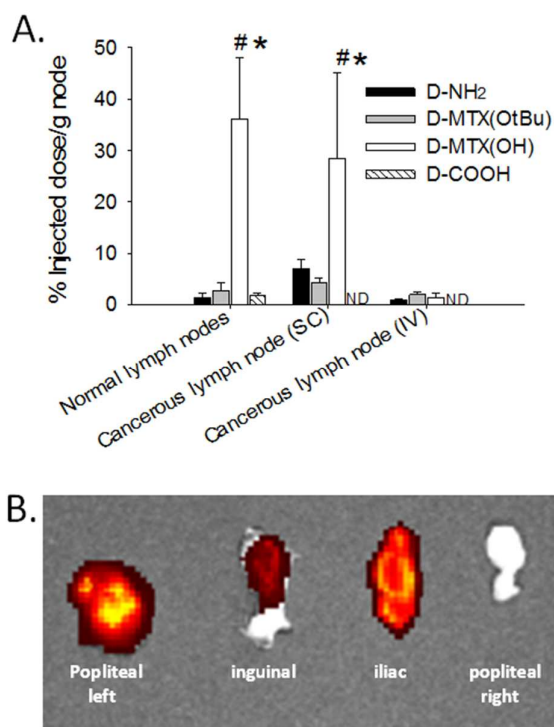
Figure 5. Panel A - Dendrimer uptake into pooled primary and secondary lymph nodes in non-tumour bearing rats after SC administration into the inner heel or primary (popliteal) tumour burdened lymph nodes after SC or IV administration. Data represents mean ± s.d. (n=3-5). * indicates $p<0.001$ vs. other dendrimers; [#] indicates $p<0.001$ vs. IV administration. ND – not determined since biodistribution in normal lymph nodes was similar to D-MTX(OtBu) and D-NH$_2$. Panel B - Ex vivo fluorescence imaging of lymph nodes 3 days after SC injection of D-MTX(OH) into the inner ipsilateral heel to primary tumour growth on a Caliper IVIS II in vivo imager.
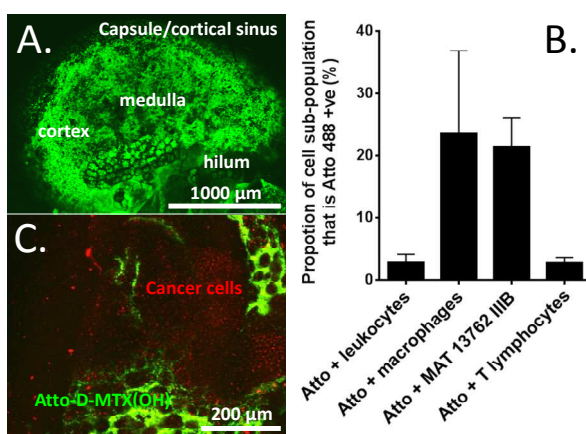
Figure 6. (A) Confocal fluorescent image (4X) of Atto488 labelled D-MTX(OH) in a popliteal lymph node 3 days after SC administration into the heel. **(B)** Proportion of cells within a tumour-bearing lymph node that were positive for Atto488-labelled D-MTX(OH) 3 days after SC administration into the inner heel of rats bearing micrometastases of MAT carcinoma. Data represents mean ± s.d (n=3-6). **(C)** Confocal fluorescent image (10X) of a popliteal lymph node bearing mCherry-expressing MAT micrometastases 3 days after SC injection of Atto488 labelled D-MTX(OH) into the inner heel of rats. Red signal is from the mCherry expressing MAT cells and the green signal is from the Atto488 label.
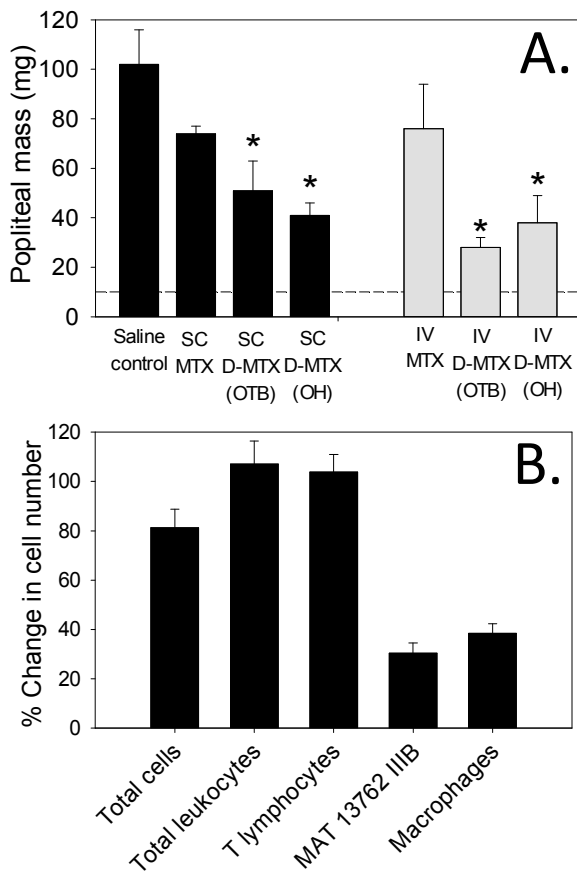
Figure 7. (A) Antitumour efficacy of MTX or MTX-conjugated dendrimers after SC administration into the inner left heel or IV administration against popliteal lymph node-resident metastases of MAT 13762 IIIB carcinoma. Dendrimers or MTX were given twice over an 8 day period beginning 12 days after the footpad injection of cancer cells. The dashed line indicates the typical mass of lymph nodes before administration of the first dose. Data represents mean ± s.e.m (n=4-7). *Indicates $p < 0.05$ cf. saline control dosed rats. **(B)** Difference in lymph node cell numbers after treatment of rats bearing popliteal lymph node-resident metastases of MAT 13762 IIIB carcinoma with SC D-MTX(OH) over an 8 day period when compared to cell numbers in the popliteal lymph node of rats treatment with saline vehicle alone. Data represents mean ± s.d. (n=3). Data for Panel B was generated in a separate group of rats to Panel A, but terminal popliteal lymph node masses did not differ significantly for either saline or SC D-MTX(OH) dosed animals between the two groups of rats.

1
2
3
4
5
6
7
8
9
10
11
12
13
14
15
16
17
18
19
20
21
22
23
24
25
26
27
28
29
30
31
32
33
34
35
36

Tables:

Table 1. Pharmacokinetic parameters for IV and SC dosed dendrimers and MTX after administration of 5 mg/kg to rats. Data represents mean ± s.d. (n=3-5).
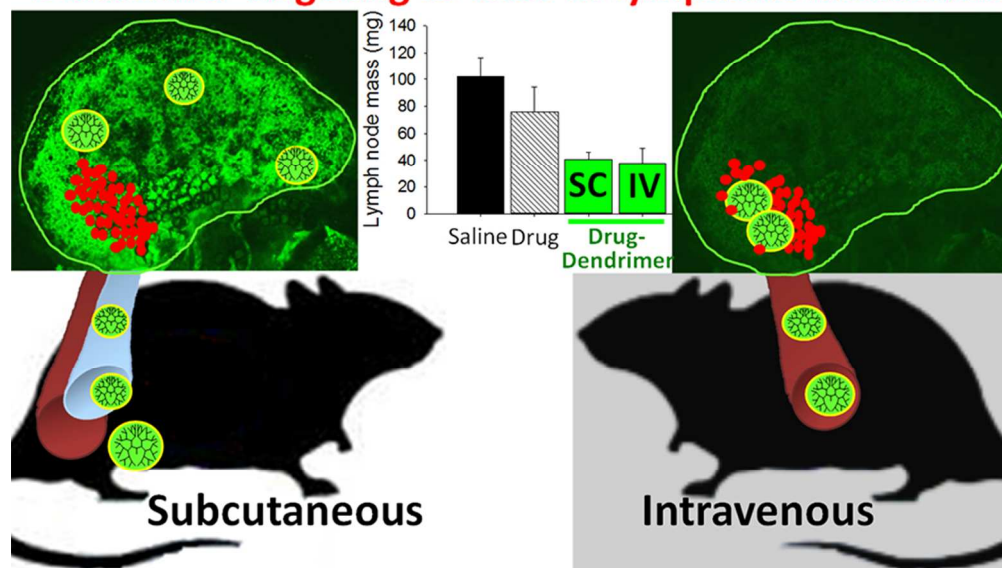
		MTX	D-NH$_2$	D-MTX(OH)	D-MTX(OtBu)	D-COOH
				IV control		
k	h^{-1}	0.43 ± 0.09	0.02 ± 0.00	2.63 ± 0.55	0.02 ± 0.00	0.02 ± 0.00
AUC$^{0-\infty}$	µg/ml.h	5.9 ± 0.2	1923 ± 210	74 ± 5	2734 ± 161	1769 ± 45
Cl	ml/h	218 ± 5	0.8 ± 0.1	20 ± 3.3	0.5 ± 0.0	0.8 ± 0.0
				SC control		
k	h^{-1}	0.34 ± 0.09	0.01 ± 0.00	ND	0.01 ± 0.00	0.02 ± 0.00
AUC$^{0-\infty}$	µg/ml.h	4.4 ± 0.5	1463 ± 607	ND	1247 ± 342	1034 ± 29
T$_{max}$	h	0.5 ± 0.0	23 ± 8	ND	21 ± 10	24 ± 0
C$_{max}$	µg/ml	3.0 ± 0.3	11.9 ± 1.2	ND	11.7 ± 3.4	13.2 ± 1.8
F	%	74 ± 8.6	76 ± 32	ND	47 ± 13	59 ± 2
				SC lymph cannulated		
k	h^{-1}	0.30 ± 0.08	ND	ND	ND	ND
T$_{max}$	h	0.4 ± 0.1	17 ± 9	ND	26 ± 3	27 ± 3
C$_{max}$	µg/ml	2.7 ± 1.3	4.8 ± 1.6*	ND	2.7 ± 2.5*	2.3 ± 1.2*
F$_{lymph}$	%	2 ± 1	19 ± 4	5 ± 2	24 ± 3	14 ± 1

ND – not determined due to the absence of an elimination phase in the plasma profile to 30 h or rapid plasma clearance following absorption

*Represents a significant difference compared to the equivalent parameter in the SC control group.

80x48mm (300 x 300 DPI)